Mathematical modeling and simulation of nanopore blocking by precipitation

M.-T. Wolfram[1], M. Burger[2] and Z. S. Siwy[3]

[1] Department of Applied Mathematics and Theoretical Physics, Wilberforce Road, CB3 0WA, Cambridge, UK

[2] Institut für Numerische und Angewandte Mathematik, Einsteinstr.62, 48149 Münster, Germany

[3] Department of Physics and Astronomy, University of California, Irvine, 210G Rowland Hall, Irvine, CA 92697, USA

E-mail: M.Wolfram@damtp.cam.ac.uk, martin.burger@wwu.de, zsiwy@uci.edu

Abstract. High surface charges of polymer pore walls and applied electric fields can lead to the formation and subsequent dissolution of precipitates in nanopores. These precipitates block the pore, leading to current fluctuations.
We present an extended Poisson-Nernst-Planck system which includes chemical reactions of precipitation and dissolution. We discuss the mathematical modeling and present 2D numerical simulations.

AMS classification scheme numbers:

Submitted to: *JPCM*

1. Introduction

Nanopores attracted a great deal of interests of scientists from various fields [1]. This is caused by the fact that nanopores are characterized by transport properties, which cannot be observed in microscale systems. Ionic and molecular selectivity [2, 3, 4, 5, 6], ion current rectification [7, 8, 9, 10, 11, 12, 13], and a diode behavior [14, 15, 16] are only a few of nanoeffects recorded with nanopores. Ionic concentrations in nanopores are often different from corresponding values in the bulk solution [17]. Surface charge of the pore walls and applied electric field can lead to increase of ionic concentrations inside a pore. If a nanopore is in contact with a solution of weakly soluble salt, ionic concentrations inside the pore can increase above the level dictated by the solubility product of this compound so that precipitates form and effectively plug the pore. This phenomenon has recently been observed in conically shaped polymer nanopores as a voltage-induced drop of the transmembrane current [18, 19]. The precipitates were found very unstable and their subsequent formation followed by dissolution resulted in ion current fluctuations in time. The characteristic feature of these voltage-induced ion current instabilities is

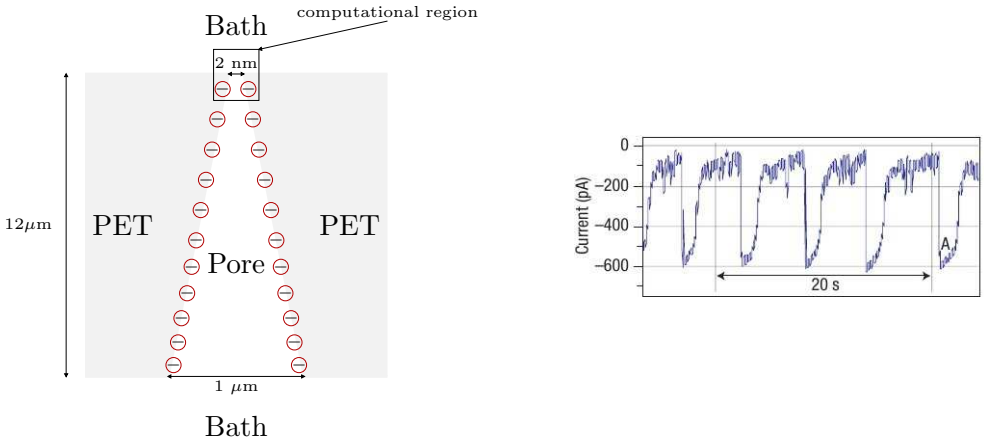

Figure 1: Left: Sketch nanopore (not in scale), right: current oscillations [19]

the existence of a voltage threshold, which defines the onset of the unstable regime. The current fluctuations have also a different shape compared to ion current switching observed in biological channels of a cell membrane [20]. The biological channels produce rectangular shaped opening and closing of the channel, indicating a very rapid kinetics of the processes responsible for the current changes. The precipitation-induced current instabilities resemble in their shape electrochemical fluctuations observed in other electrochemical systems [21]. Namely, the current spikes have a very asymmetric shape: there is a quick increase of the current followed by much slower process of pore closing, which we attribute to the nanoprecipitates formation. The current instabilities produced by conical nanopores are also very periodic, especially at higher applied voltages. The oscillating conical nanopores produce the fastest electrochemical oscillations observed so far, offering frequencies between fractions of Hz up to tens of Hz.

Different approaches can be found in literature to describe particular features of nanopores with the desired complexity, i.e. the stationary Poisson Nernst Planck (PNP) equations to calculate the current through nanopores [17, 22], a coupled Monte-Carlo PNP model to describe the anomalous mole fraction effect [23], or Molecular Dynamics simulation to model the ion current rectification in silica nanopores [24] and polymer [25]. Few results can be found in the mathematical literature on mathematical models for precipitation and dissolution, e.g. crystal dissolution and precipitation in porous media [26, 27].

In this publication we present the first application of the PNP equations coupled with chemical reactions applied to ion current instabilities observed in nanoporous systems. The model gives insight into the kinetics and microscopic picture of the nanopore with transient precipitates. We believe that the developed approach can be applied to other nanoporous systems in which current instabilities have been observed.

2. Mathematical modeling of nanopores - the extended Poisson-Nernst-Planck equations

Our proposed mathematical model is based on the 2D PNP equations, which assume that the main driving forces for the ions are the diffusion and the electrostatic interaction with other ions and the surface charges on the pore walls. The PNP equations are a standard model for electrodiffusion of ions, cf. [28], their application to ion channels has been discussed e.g. in [29, 30, 31], and to nanopores e.g. in [22, 17]. The general formulation of the PNP equations is given by:

$$\operatorname{div}(\varepsilon \nabla V) = e \sum_{k=0}^{m} z_k \rho_k \tag{1a}$$

$$\frac{\partial \rho_k}{\partial t} = \operatorname{div} J_k \qquad \forall k = 1, \dots m \tag{1b}$$

$$J_k = -\frac{1}{k_B T} D_k(x) \rho_k \nabla \mu_k \qquad \forall k = 1, \dots m \tag{1c}$$

$$\mu_k = \mu_k^0 + z_k e V + k_B T \log(\rho_k) + \mu_k^{ex} \quad \forall k = 1, \dots m, \tag{1d}$$

where ρ_k is the concentration of the k-th ionic species and V the electric potential. The total number of different species present in the system is denoted by m. We refer to D_k as the diffusion coefficient of every species, z_k is the corresponding valence. The parameter k_B is the Boltzmann constant, T denotes the temperature, ε the dielectric coefficient and e the elementary charge. We refer to μ_k in $(1d)$ as the electrochemical potential, which includes electrostatic interaction (second term), diffusion (third term), external forces via a potential μ_k^0 and finite size effects via μ_k^{ex} (excess chemical potential). The potential μ_k^{ex} can be calculated e.g. using density functional theory (DFT) for fluids [29] or mean spherical approximations, see [31].

The general PNP equations $(1a)$-$(1d)$ serve as a basis for our extended mathematical model including precipitation and dissolution. The first numerical simulations of the PNP equations by Cervera et al. [17] showed good agreement with the experimental data for $\mu_k^{ex} = 0$. In our first model we will thus neglect the effects of the excess chemical potential μ_k^{ex} and set it to zero, a stronger impact of the excess chemical potential is expected for smaller pores however.

As an example, we discuss the formation of cobalt hydrogen phosphate $CoHPO_4$ in a system of KCl, $CoCl_2$, K_2HPO_4, and KH_2PO_4. We do not consider formation of $Co_3(PO_4)_2$ whose presence was found in bulk solutions containing $CoSO_4$ and Na_2HPO_4 (see [32]). The salt $Co_3(PO4)_2$ has an extremely low solubility product of the order of magnitude of 10^{-35}. We think that $Co_3(PO4)_2$ is not formed in our nanopores since we found that very weekly soluble compounds e.g. $Zn(OH)_2$ ($K_{sp} = 4 \times 10^{-7}$ $(\mathrm{mol/l})^3$) caused a complete and permanent blockage of the pore so that no current instabilities were observed. Existence of pore openings and closings is therefore treated as indirect evidence that only salts with intermediate values of solubility product can be formed in the system with Co^{2+} and HPO_4^{2-}.

Precipitation can occur if

$$K_{sp} < a_{\mathrm{Co^{2+}}} a_{\mathrm{HPO_4^{2-}}}, \tag{2}$$

where $a_{Co^{2+}}$ and $a_{HPO_4^{2-}}$ denotes the activity of the ionic species in equilibrium and K_{sp} the solubility equilibrium constant. On the other hand if $K_{sp} > a_{\mathrm{Co^{2+}}}\ a_{\mathrm{HPO_4^{2-}}}$ then $\mathrm{CoHPO_4}$ dissolves into its component parts $\mathrm{Co^{2+}}$ and $\mathrm{HPO_4^{2-}}$. The activity of a species is directly proportional to its concentration, i.e.

$$a_{\mathrm{Co^{2+}}} = \gamma_{\mathrm{Co^{2+}}} \rho_{\mathrm{Co^{2+}}} \quad \text{and} \quad a_{\mathrm{HPO_4^{2-}}} = \gamma_{\mathrm{HPO_4^{2-}}} \rho_{\mathrm{HPO_4^{2-}}},$$

where $\gamma_{\mathrm{Co^{2+}}}$ and $\gamma_{\mathrm{HPO_4^{2-}}}$ denote the activity coefficients, $\rho_{\mathrm{Co^{2+}}}$ and $\rho_{\mathrm{HPO_4^{2-}}}$ the concentrations. Note that the activity of a species depends heavily on the temperature and that the activity of a pure solid equals one by definition. Different models for the calculation of the activity coefficients can be found in literature, we concentrate on the Brønsted-Guggenheim-Scatchard specific interaction theory [33, 34, 35].

The rate of a chemical reaction can be quantified by the precipitation and dissolution rate k_p and k_d respectively. Then the formation of $\mathrm{CoHPO_4}$ can be written as the following system of ordinary differential equations (in absence of other effects)

$$\frac{\partial \rho_{\mathrm{Co^{2+}}}}{\partial t} = -k_p \rho_{\mathrm{Co^{2+}}} \rho_{\mathrm{HPO_4^{2-}}} + k_d \rho_{\mathrm{CoHPO_4}} \tag{3a}$$

$$\frac{\partial \rho_{\mathrm{HPO_4^{2-}}}}{\partial t} = -k_p \rho_{\mathrm{Co^{2+}}} \rho_{\mathrm{HPO_4^{2-}}} + k_d \rho_{\mathrm{CoHPO_4}} \tag{3b}$$

$$\frac{\partial \rho_{\mathrm{CoHPO_4}}}{\partial t} = k_p \rho_{\mathrm{Co^{2+}}} \rho_{\mathrm{HPO_4^{2-}}} - k_d \rho_{\mathrm{CoHPO_4}} \tag{3c}$$

with given initial concentrations for $\rho_{\mathrm{Co^{2+}}}$, $\rho_{\mathrm{HPO_4^{2-}}}$ and $\rho_{\mathrm{CoHPO_4}}$.

These reaction equations can be included into the PNP system. Let ρ_1 and ρ_2 denote the concentration of the soluble ions participating in the chemical reaction (e.g. $\mathrm{Co^{2+}}$ and $\mathrm{HPO_4^{2-}}$ ions), ρ_3 the concentration of the solid species (e.g. cobalt hydrogen phosphate $\mathrm{CoHPO_4}$) and $\rho_4 \dots \rho_m$ other ions present in the solution. Then the extended PNP system reads

$$-\mathrm{div}\,(\varepsilon \nabla V) = e\left(z_1\rho_1 + z_2\rho_2 + \sum_{k=4}^{m} z_k \rho_k\right) \tag{4a}$$

$$\frac{\partial \rho_1}{\partial t} = \mathrm{div}\left[D_1(\rho_3)\left(\nabla \rho_1 + z_1 \frac{e}{k_B T}\rho_1 \nabla V\right)\right] - \\ - a(x) k_p \rho_1 \rho_2 + (1 - a(x)) k_d \rho_3 \tag{4b}$$

$$\frac{\partial \rho_2}{\partial t} = \mathrm{div}\left[D_2(\rho_3)\left(\nabla \rho_2 + z_2 \frac{e}{k_B T}\rho_2 \nabla V\right)\right] - \\ - a(x) k_p \rho_1 \rho_2 + (1 - a(x)) k_d \rho_3 \tag{4c}$$

$$\frac{\partial \rho_3}{\partial t} = \mathrm{div}\left[D_3\left(\rho_3\right)\left(\nabla \rho_3\right)\right] + a(x) k_p \rho_1 \rho_2 - (1 - a(x)) k_d \rho_3 \tag{4d}$$

$$\frac{\partial \rho_k}{\partial t} = \mathrm{div}\left[D_k\left(\rho_3\right)\left(\nabla \rho_k + z_k \frac{e}{k_B T}\rho_k \nabla V\right)\right] \qquad k = 4, \dots m. \tag{4e}$$

Note that except the reduced mobility due to formation of precipitates we do not include any finite size effects or external potentials at this point, i.e. $\mu_k^{ex} = \mu_k^0 = 0$ in $(1d)$. The

diffusion coefficients $D_i,\ i = 1, \dots m$ depend on the density of the solid ρ_3, modeling the blocking of the pore. We model them of the form

$$D_k(\rho_3(x), x) = \tilde{D}_k(x) m(\rho_3(x)) \quad \text{with} \quad m(\rho) = 2\frac{e^{-\gamma\rho}}{1 + e^{-\gamma\rho}}, \tag{5}$$

where $\tilde{D}_k(x)$ denotes the diffusivity in the pore and bath. Note that the function $m(\rho(\cdot))$ decreases exponentially with ρ_3, i.e. the higher the concentration of the precipitate the lower the diffusivity. The dependence of diffusion coefficients on the precipitate concentration can be thought of as a limit of a diffusion coefficient depending on the total volume occupied by all species such as in the modified PNP model with size effects discussed in [36].The coefficient $a(x)$ is determined by the activity of the solution

$$a(x) = \begin{cases} 1 & a_1(x)a_2(x) > K_{sp} \\ 0 & a_1(x)a_2(x) < K_{sp} \end{cases}$$

where $a_1(x)$ and $a_2(x)$ are the activities of ρ_1 and ρ_2 respectively and K_{sp} is the solubility constant. The carboxyl charges on the inside of the pore wall are modeled using Neumann boundary conditions, namely

$$\varepsilon \frac{\partial V}{\partial n} = \sigma \quad \forall x \in \Gamma_p. \tag{6}$$

For the different species we fix the applied voltage U and the ionic concentrations in the bath

$$\begin{aligned} \rho_k &= \eta_k \quad \forall x \in \Gamma_D, \\ V &= U \quad \forall x \in \Gamma_D. \end{aligned}$$

On the remaining part of the boundary we model insulation using homogeneous Neumann boundary conditions. Based on Equation (6), we choose the following scaling

$$x = L x_s \qquad V = \tilde{V} V_s \qquad \sigma = \tilde{\sigma}\sigma_s,$$

where L denotes the typical length, $\tilde{V}$ the typical voltage and $\tilde{\sigma}$ the typical density of surface charge density . Then the scaled Neumann boundary condition Equation (6) is given by

$$\left(\frac{\varepsilon\tilde{V}}{\tilde{\sigma}L}\right)\frac{\partial V_s}{\partial n_s} = \sigma_s.$$

Therefore we choose the effective parameter λ to be

$$\lambda^2 = \frac{\varepsilon\tilde{V}}{L\tilde{\sigma}}.$$

Then the scaled system $(4a)$-$(4e)$ reads as (omitting the subscript s)

$$-\lambda^2 \Delta V = \kappa[(z_1\rho_1 + z_2\rho_2) + \sum_{k=4}^{m} z_k\rho_k] \tag{7a}$$

$$\begin{aligned} \frac{\partial \rho_1}{\partial t} &= \operatorname{div}\left[D_1(\rho_3)\left(\nabla\rho_1 + cz_1\rho_1\nabla V\right)\right] - \\ &\quad - a(x)k_p\rho_1\rho_2 + (1 - a(x))k_d\rho_3 \end{aligned} \tag{7b}$$

$$\frac{\partial \rho_2}{\partial t} = \operatorname{div}\left[D_2(\rho_3)\left(\nabla \rho_2 + c z_2 \rho_2 \nabla V\right)\right] -$$

$$- a(x) k_p \rho_1 \rho_2 + (1 - a(x)) k_d \rho_3 \tag{7c}$$

$$\frac{\partial \rho_3}{\partial t} = \operatorname{div}\left[D_3\left(\rho_3\right)\left(\nabla \rho_3\right)\right] + a k_p \rho_1 \rho_2 - (1-a) k_d \rho_3 \tag{7d}$$

$$\frac{\partial \rho_k}{\partial t} = \operatorname{div}\left[D_k\left(\rho_3\right)\left(\nabla \rho_k + c z_k \rho_k \nabla V\right)\right] \tag{7e}$$

where $\kappa = \frac{eL\tilde{\rho}}{\tilde{\sigma}}$, $c = \frac{eV}{k_B T}$ and $\tilde{\rho}$ denotes the typical concentration of the ionic species.

3. Numerical scheme

We use the following Gummel-type procedure to solve the PNP equations (7*a*)-(7*e*) at every time step $t = t_j$. Here V_j and $\rho_{k,j}$ denote the potential and the k-th ionic species at time $t = t_j$ respectively.

- Solve the Poisson equation (7*a*) for the potential V_j
- Solve the Nernst-Planck equations (7*b*)-(7*e*) for $\rho_{k,j}$ in an iterative manner using the potential V_j.

The Poisson equation (7*a*) can be solved using a standard hybrid discontinuous Galerkin (DG) method. The Nernst-Planck equations (7*b*)-(7*e*) are solved using a semi-implicit discretization in time. For the sake of readability we only state the semi-discrete equation for ρ_1 given by

$$\frac{\rho_{1,j} - \rho_{1,j-1}}{\Delta t} + \operatorname{div}\left[D_1\left(\rho_{3,j-1}\right)\left(\nabla \rho_{1,j} + c z_1 \rho_{1,j} \nabla V\right)\right] =$$

$$\left(-a(x) k_p(x) \rho_{1,j-1} \rho_{2,j-1} + \left(1 - a(x)\right) k_d \rho_{3,j-1}(x)\right). \tag{8}$$

Here Δt denotes the time steps $\Delta t = t_j - t_{j-1}$. Equations (7*b*)-(7*e*) are solved using a mixed stabilized DG method introduced in [37]. For a detailed presentation of the numerical scheme we refer to [38].

4. Simulations

Nanopores have different length scales - the length of the pore is in the micrometer range, the narrow opening in the nanometer range, resulting in a multiscale problem. Since the plugging of the pore happens at its narrow tip, we consider only the narrow opening part in our calculations (see Figure 1).
We choose a tapered cone of length $\tilde{L} = 50$ nm with opening diameters $d_1 = 2$ nm and $d_2 = 3$ nm. These diameters correspond to the opening angle $\theta \approx 1^\circ$ of actual nanopores. The computational geometry consists of the small cone tip as well as two attached conical shaped bath regions. The typical length is set to $L = 1$ nm, the typical concentration $\tilde{\rho} = 1$ mM and the typical surface charge to $\tilde{\sigma} = 1 \frac{\mathrm{e}}{\mathrm{nm}^2}$.
The generalized PNP system (7*a*)-(7*e*) involves five species, the dissolved ions Co^{2+},

j	1	2	3	4	5
Species	Co	HPO_4^{2-}	$CoHPO_4$	Cl	K
Charge	2e	-2e	0	-e	e
Left bath ρ_j	0.2 mM	0 mM	0 mM	0.4 mM	0 mM
Right bath ρ_j	0 mM	1 mM	0 mM	0 mM	2 mM

Table 1: Values for the Dirichlet boundary conditions

K^+, Cl^- and HPO_4^{2-} as well as the precipitate $CoHPO_4$. The bulk solubility product $K_{sp} = 2 \times 10^{-7}(\text{mol}/l)^2$ is taken from [39], the scaled precipitation and dissolution rates are chosen to be $k_p = k_d = 2$. The dissolution and precipitation rate are chosen such that the length scales of the plugging and dissolution fits the experimental data. If the dissolution rate k_d is too large the concentrations might become negative and the numerical scheme unstable.
The boundary conditions for the concentrations are chosen such that the the charge neutrality condition $\sum_{k=0}^{m} z_k \rho_k = 0$ is satisfied (see Table 1). The initial conditions are set to

$$\rho_k(x,0) = \begin{cases} \eta_{k,r} & \text{for all } x \text{ in the right bath} \\ \eta_{k,l} & \text{for all } x \text{ in the left bath} \\ 0 & \text{inside the pore} \end{cases} \tag{9}$$

where $\eta_{k,r}$ and $\eta_{k,l}$ denote the Dirichlet boundary values respectively.
Figure 2 illustrates the formation of a plug in the nanopore (only the very narrow tip and the parts of the attached bath are shown in the picture). The plug originates in the center of the narrow tip and accumulates below the narrow tip. It causes a decrease in the diffusivity, see equation 5, as well as in the measured current (see Figure 3). The plugging of the pore happens on the same time scale as in the experiments, it takes about 5 ms until the plug starts to dissolve. The decrease in the current is of the same order of magnitude as the decrease in the experiments. The current model is not able to reproduce the fast dissolution of the plug or multiple openings and closings of the pore. Therefore we can't see any increase of the current in Figure 3 after the plug dissolves.

5. Conclusions and further work

We presented an extended PNP model which provides the first insight into the kinetics of formation and dissolution of precipitates inside a single conically shaped nanopore. First numerical simulations show good agreement with experimental data, i.e. the plug formation happens on same time scale as observed experimentally. Our studies also raise a number of interesting questions e.g.

- What are other possible models for the formation and dissolution of a plug ?

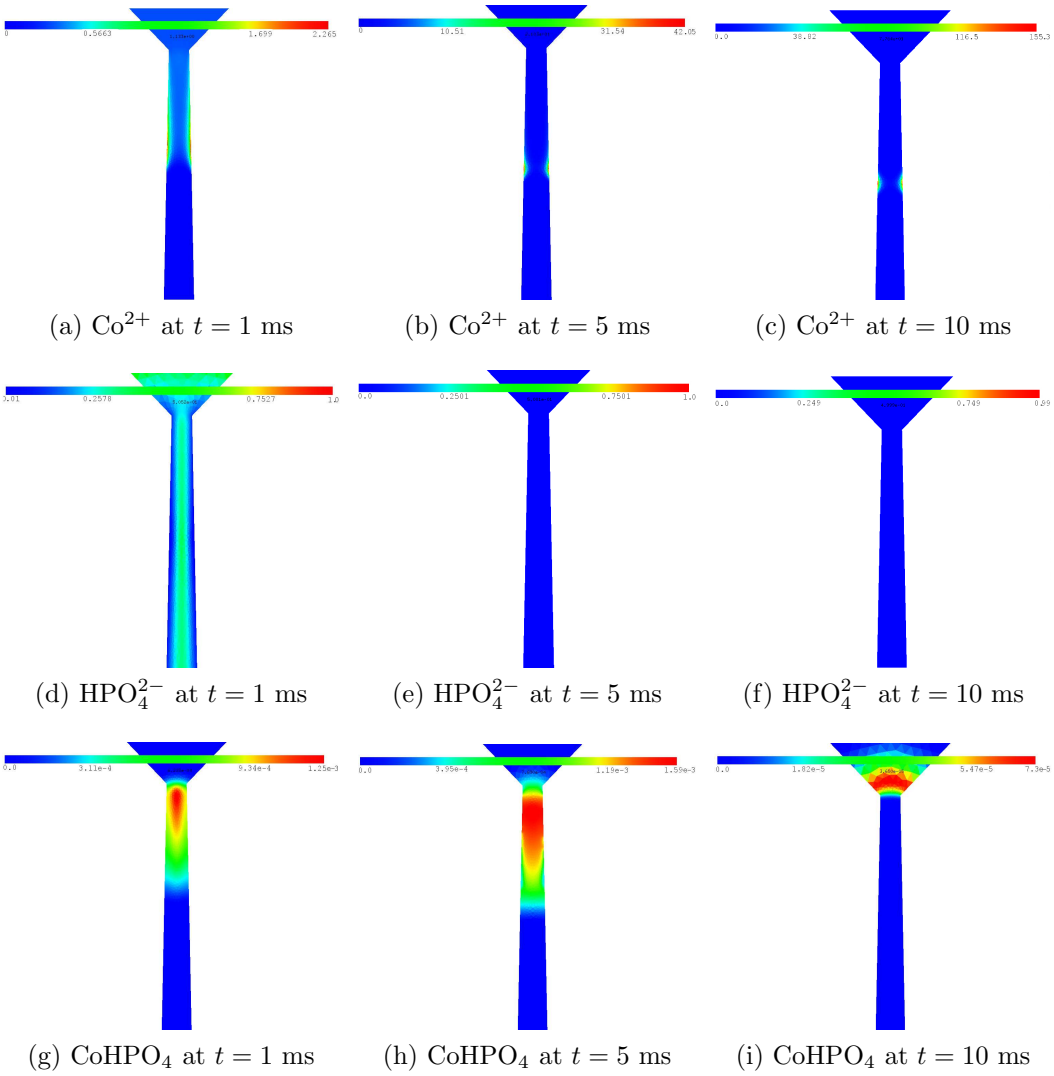

(a) Co^{2+} at $t = 1$ ms (b) Co^{2+} at $t = 5$ ms (c) Co^{2+} at $t = 10$ ms

(d) HPO_4^{2-} at $t = 1$ ms (e) HPO_4^{2-} at $t = 5$ ms (f) HPO_4^{2-} at $t = 10$ ms

(g) $CoHPO_4$ at $t = 1$ ms (h) $CoHPO_4$ at $t = 5$ ms (i) $CoHPO_4$ at $t = 10$ ms

Figure 2: Formation of a plug as a function of time; the range of the scaled concentrations are (a) [0mM, 2.265mM], (b) [0mM, 42.05mM] , (c) [0mM, 155.3mM], (d) [0mM, 1mM], (e) [0mM, 1mM], (f) [0mM, 0.99mM], (g) [0mM, $1.25e^{-3}$mM], (h) [0mM, $1.59e^{-3}$mM], (i) [0mM, $7.3e^{-5}$mM]

- What are appropriate values for the precipitation and dissolution rate of the precipitates in a nanopore ?
- Do the solubility products in nanopores differ from their values in the bulk ?
- What is the chemical composition of the formed precipitate ?

These questions pose further challenges for mathematicians and experimentalists. Different mathematical approaches could apply various thresholds in order to describe the formation of the plug. In our calculations, we indeed used the value of solubility product determined for a macroscopic solution. It is indeed an oversimplification of the system since dissociation and ionization constants have already been shown to be different in track-etched nanopores compared to macroscopic films and bulk solutions [40]. The

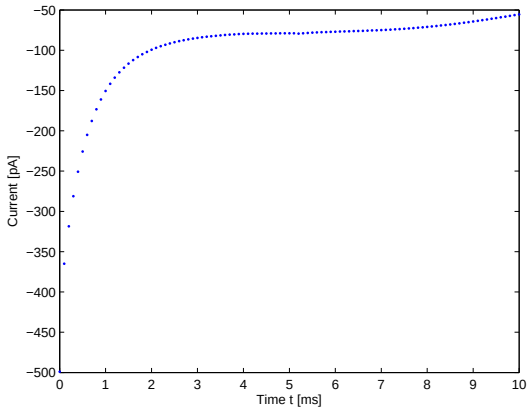

Figure 3: Decrease of ion current in time due to formation of nanoprecipitates at the tip of the pore

applied electric field can further change the kinetics of precipitation formation. The purpose of the modeling is however to indicate that already the simplest treatment of the system with bulk values of solubility products and one precipitating salt is sufficient for numerical reproducing of the current instabilities.

Another interesting feature is the asymmetric shape of the current fluctuations: the pore opening occurs on a much faster time scale than the plugging. This observation might point to yet another mechanism for the pore opening. It is possible that the precipitate formation increases the pressure inside the pore, which leads to the precipitate being "ejected". Formation of nanoparticles with nanopores was indeed observed in a multi-pore system but no theoretical description for this phenomenon on the nanoscale is yet available [41]. In order to study this option, the presented model would have to be complemented by additional equations, e.g. by coupling PNP with the Navier-Stokes equations or at least by assuming that the diffusion coefficient D_k depends on the pressure.

Formation of nanoparticles also calls for determination of their chemical composition, which is planned in the future. Membranes containing many pores will be used in the experiments so that sufficient amount of precipitates will allow one to study their composition by e.g. energy-dispersive x-ray spectroscopy (EDS), and x-ray diffraction (XRD).

References

[1] Dekker C 2001 *Nat. Nanotech.* **2** 209-215
[2] Plecis A, Schoch R B, and Renaud P 2005 *Nano Lett.* **5** 1147-55
[3] Nishizawa , Martin C R, and Menon V P 1995 *Science* **268** 700-702
[4] Vlassiouk I, Smirnov S, and Siwy Z S 2008 *Nano Lett.* **8** 1978-85
[5] Kohli P, Harrell C, Cao C Z, Gasparac R, Tan W, and Martin C R 2004 *Science* **305** 984-986

[6] Howorka S, and Siwy Z S 2009 *Chem. Soc. Rev.* **38** 2360-84
[7] Wei C, Bard J and Feldberg S W 1997 *Anal. Chem.* **69** 4627-46
[8] Apel P Y, Korchev Y E, Siwy Z, Spohr R and Yoshida M 2001 *Nucl. Instrum. Methods Phys. Res. B* **184** 337-346
[9] Siwy Z S, and Fulinski A 2002 *Phys. Rev Lett.* **89** 1981031-4
[10] While H S, and Bund A 2008 *Langmuir* **24** 12062-67
[11] Umehara S, Pourmand N, Webb C D, Davis R W, Yasuda K, and Karhanek M 2006 *Nano Lett.* **6** 2486-92
[12] Siwy Z S, Heins E, Harrell C C, Kohli P, and Martin C R 2004 *J. Am. Chem. Soc.* **126** 10850-51
[13] Siwy Z S, and Howorka S 2010 *Chem. Soc. Rev* DOI 10.1039/b909105j
[14] Vlassiouk I, and Siwy Z S 2007 *Nano Lett.* **7** 552-56
[15] Karnik R, Duan C H, Castelino K, Daiguji H, and Majumdar A 2007 *Nano Lett.* **7** 547-51
[16] Cheng L J, and Guo L J 2009 *ACS Nano* **3** 575-84
[17] Cervera J, Schiedt B, and Ramírez P 2005 *EPL (Europhysics Letters)* **71** 35–41
[18] Siwy Z, Powell M R, Petrov A, Kalman E, Trautmann C, and Eisenberg R S (2006) *Nano Lett.* **6** 1729-34
[19] Powell M R, Sullivan M, Vlassiouk I, Constantin D, Sudre O, Martens C C, Eisenberg R S and Siwy Z S 2008 *Nature Nanotech.* **3** 51-57
[20] Hille B 2001 *Ion channels of excitable membranes* Sinauer Associates
[21] Degn H 1968 *Transaction of the Faraday Society* **64** 1348-1358
[22] Cervera J, Schiedt B, Neumann R, Mafe S, and Ramirez P 2006 *J. Chem. Phys.* **124** 104706
[23] Gillespie D, Boda D, He Y, Apel P and Siwy Z S 2008 *Biophys. J.* **95** 609-19
[24] Cruz-Chu E R, Aksimentiev A and Schulten K 2009 *Journal of Phys. Chem. C* **113** 1850-62
[25] Cruz-Chu E R, Ritz T, Siwy Z S and Schulten K 2009 *Faraday Discussion* **43** 1-16
[26] Devigne V M, Pop I S, van Duijn C J and Clopeau T 2008 *SIAM J. Numer. Anal.*, **46** 895–919
[27] Maisse E and Pousin J 1997 *J. Comput. Appl. Math.*, **82** 279–90
[28] Rubinstein I 1990 *Electro-Diffusion of Ions* (Society for Industrial and Applied mathematics)
[29] Gillespie D, Nonner W, and Eisenberg R S 2002 *J. Phys.: Condens. Matter* **14** 12129–45
[30] Gillespie D, Nonner W, and Eisenberg R S 2003 *Phys. Rev. E* **68** 031503
[31] Nonner W, Catacuzzeno L and Eisenberg R S 2000 *Biophys. J.* **79** 1976-92
[32] Ishikawa T and Matijevic E 1988 *J. Colloid Interface Sci.* **123** 122-128
[33] Guggenheim E A 1934, *Phil. Mag* **19** 588-643
[34] Scatchard G 1976, *Equilibrium in Solutions: Surface and Colloid Chemistry* (Havard University Press)
[35] Ciavatta L 1980, *Annali di Chimica* **70** 551-67
[36] Burger M, Schlake B 2010, Nonlinear Poisson-Nernst-Planck equations for flux through confined geometries, Preprint.
[37] Egger H and Schöberl J 2009 *IMA. J. Num. Anal.*
[38] Wolfram M.-T. 2008 *Forward and Inverse Solvers for Electrodiffusion Systems* (PhD Thesis, University of Linz)
[39] Dean J A 1998 *Lange's Handbook of Chemistry* (McGraw-Hill Professional)
[40] Korchev Y E, Bashford C L, Alder G M, Apel P Y, Edmonds D T, Lev A A, Nandi K, Zima A V and Pasternak C A (1997) *FASEB* **11** 600-608
[41] Guo P, Martin C R, Zhao Y, Ge J and Zare R N (2010) *Nano Letters* **10** 2202-2206

Acknowledgments

MB has been supported by the Volkswagen Stiftung, Grant Nr. I/83-928. MTW has been supported by Award No. KUK-I1-007-43, made by King Abdullah University of Science and Technology (KAUST). ZS was supported by the National Science

Foundation (CMMI 0825661). The authors thank R.S.Eisenberg (Rush Medical University) for useful and stimulating discussions.